Variation of structural and hyperfine parameters in nanoparticles of Cr-substituted Co-Zn ferrites

Ram Kripal Sharma,[1] Varkey Sebastian,[1,2] N. Lakshmi,[1] K. Venugopalan,[1] V. Raghavendra Reddy,[3] and Ajay Gupta[3]
[1]*Department of Physics, Mohanlal Sukhadia University, Udaipur 313001, India*
[2]*Department of Physics, Nirmalagiri College, Kerala 670701, India*
[3]*UGC-DAE Consortium for Scientific Research, Khandwa Road, Indore 452017, India*
(Received 28 November 2006; published 19 April 2007)

The effect of Cr substitution into nanocrystalline Co-Zn ferrite prepared by the chemical coprecipitation method has been studied. Mössbauer studies at a temperature (20 K) well below the blocking temperatures of the samples show that Cr goes preferentially into the octahedral *B* site and that the hyperfine fields at both *A* and *B* sites decrease with increase in Cr concentration. Based on the cation distribution obtained from fitting Mössbauer spectra, structural parameters such as lattice parameters, site bond and edge lengths, and the oxygen parameter *u* have been calculated. The trend of theoretically calculated lattice parameter with Cr content matches well with the experimentally obtained values.

DOI: 10.1103/PhysRevB.75.144419 PACS number(s): 75.75.+a, 81.16.Be

I. INTRODUCTION

Nanocrystalline ferrite systems have been the topic of intense research in recent years due to the wide possibilities of use in technological applications that require miniaturization as in high-density data storage. In ferrites, the magnetic properties are mainly dependent on the type of metal ions and their distribution between the tetrahedral *A* and octahedral *B* sites.[1] Hence, the tuning of magnetic properties requires a thorough understanding of the influence of preparation methods, substitution, and thermal treatments on the cation distribution. In ferrites of the same composition, the physical properties are also size dependent, since the properties of nanosystems are largely determined by interparticle spacing and surface-to-volume ratio.[2]

The mixed spinel $Co_{0.5}Zn_{0.5}Fe_2O_4$ is well suited for the study of size effects, since Co and Zn have strong preferences for the octahedral and tetrahedral sites, respectively. According to these preferences, the cation distribution should be $(Zn_{0.5}Fe_{0.5})[Co_{0.5}Fe_{1.5}]O_4$. However, in nanoparticles, various effects arising due to small particle sizes[3] may result in a different distribution. The spinel structure also allows introduction of different metallic ions, which can change the magnetic and electrical properties considerably.[4,5] Magnetic properties in these materials such as magnetic anisotropy, coercivity, appearance of superparamagnetism, and variation in hyperfine fields can be tailored by simple substitution of other magnetic and/or nonmagnetic ions.[6]

A study of the hyperfine fields gives valuable information about the Fe site occupancy and strength of interactions, which can be used to estimate the cation distribution, thus enabling a comparative study of the differences between bulk system and nanosystem of the same nominal composition. Recently, we had reported the magnetic properties of a bulk $Cr_xCo_{0.5-x}Zn_{0.5}Fe_2O_4$ system prepared by the chemical coprecipitation method and studied using Mössbauer effect.[7] In the present study, we report the effect of particle size on the properties of a nanosystem of the same composition prepared under identical conditions. At room temperature, this nanosystem is superparamagnetic.[8] To compare the magnetic hyperfine fields at Fe sites in the nanosized particles to that in the bulk, Mössbauer measurements have been made at a temperature much less than the blocking temperature.

II. EXPERIMENT

Nanoparticles of $Cr_xCo_{0.5-x}Zn_{0.5}Fe_2O_4$ were synthesized by a chemical coprecipitation method.[8] The precipitate was dried at 373 K for 24 h and subsequently annealed at 573 K for 24 h to obtain the nanosamples. To confirm the stoichiometry of the samples, energy dispersive x-ray (EDX) analysis was done on all the samples. EDX spectra show that the stoichiometry of the samples is within ±2% error of the desired ratio. X-ray diffractograms (XRD) were obtained using a Rigaku Miniflex x-ray diffractometer (30 kV, 15 mA, Ni filter) with Cu $K\alpha$ radiation. The average crystallite size *d* was calculated from the broadening of the most intense (311) peak in the XRD spectrum. Correction for instrumental broadening was done using the expression

$$\beta = B - b. \tag{1}$$

Here, *B* is the full width at half maximum (FWHM) obtained by fitting a Lorentzian (Cauchy) profile to individual XRD peak and *b* is the instrumental broadening determined from an x-ray pattern of standard silicon sample used for instrumental calibration. The average crystallite size was obtained using the Scherrer equation $t=0.9\lambda/(\beta\cos\theta)$ [where *t* is the crystallite size, λ is the x-ray wavelength, and θ is the position of the (311) peak in the XRD]. Lattice parameter a_0 was obtained using the powder–diffraction package[9] (PDP 1.1) program. Using the INDEX subroutine available in the program, the spectrum was checked to confirm the cubic structure. Appropriate value of $s=h^2+k^2+l^2$ was determined, and the lattice parameter calculated using the equation

$$\frac{\sin^2\theta}{s} = \frac{\lambda^2}{4a_0^2}. \tag{2}$$

Mössbauer measurements were made with a 25 mCi Co^{57} (Rh) source at 20 K. Velocity calibration was done using

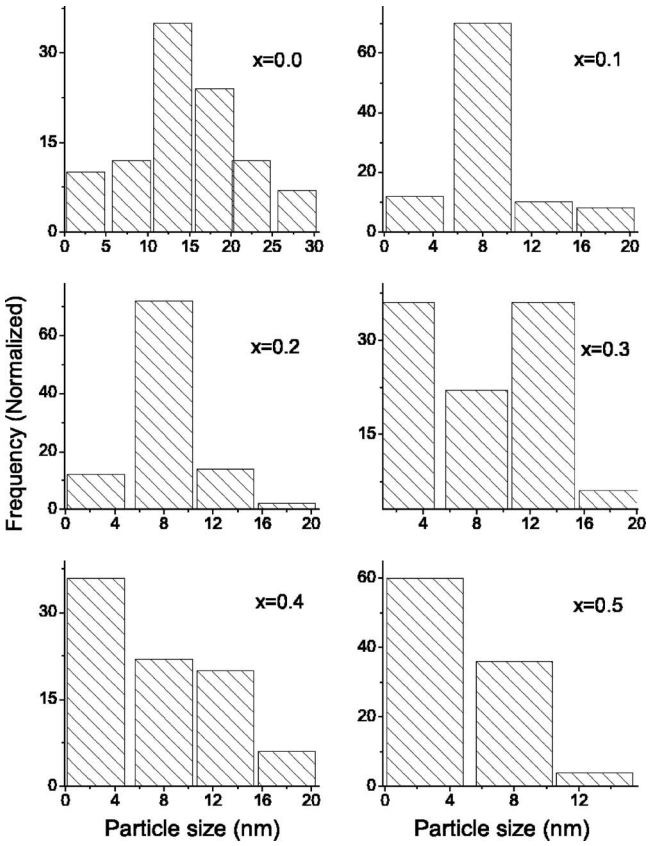

FIG. 1. Particle size distribution in $Cr_xCo_{05-x}Zn_{0.5}Fe_2O_4$ for different values of x.

metallic iron foil. Mössbauer spectra were fitted using a standard program that fits for Lorentzians.[10]

III. RESULTS AND DISCUSSIONS

A. Variation of particle size and lattice constant with Cr concentration

A systematic decrease in the particle size in the nanosystem is observed with an increase in Cr concentration. The average particle size of the samples has been determined using the Scherrer equation and corroborated by transmission electron microscopy (TEM). Figure 1 gives the particle size distribution for the samples determined from TEM. The size for $x=0.0$ is around 6.5 nm and decreases to approximately 2.5 nm for $x=0.5$,[8] suggesting that the presence of chromium inhibits crystal growth. In coprecipitation methods, the crystal growth depends on various parameters, the most important being the molecular concentration of the constituents approaching the surface of the crystal during the process of growth. The liberation of latent heat at the surface makes the local temperature higher than the average temperature of the solution. The surface temperature affects the local molecular concentration at the crystal surface, and hence the crystal growth.[11] The trend of crystallite size in the present series suggests that the formation of chromium-zinc ferrite is more exothermic compared to cobalt-zinc ferrite.[12]

The dependence of grain size on chromium concentration may also be related to the site preferences of Cr, Zn, and Co

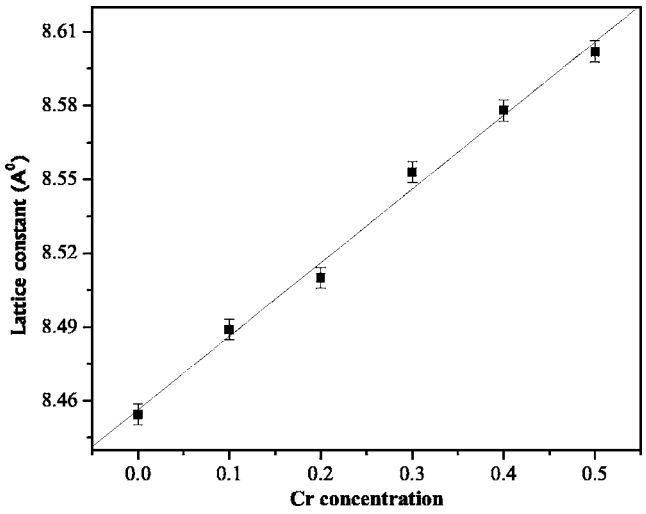

FIG. 2. Variation of lattice constant for nanoparticles of $Cr_xCo_{05-x}Zn_{0.5}Fe_2O_4$ with Cr concentration. The line is a linear fit to the experimental points.

ions in spinel structure of ferrites.[13,14] It is well known that Zn ions in the spinel structure have very strong preference for tetrahedral A sites, while Co and Cr ions have a strong preference for octahedral B sites. It has been reported[15] that when ions with strong site preferences are substituted into a ferrite, the particle size decreases with an increase in the content of the substituting ion. This is attributed to the reduced flexibility of substitution into the available sites during particle growth, thus limiting the nucleation process and size. Mössbauer studies in the present series confirm the preferential substitution of Cr into the octahedral B sites, and so the decrease in particle size with increase in Cr content can be partially attributed to the strong octahedral site preference of Cr in $Cr_xCo_{0.5-x}Zn_{0.5}Fe_2O_4$.

The lattice constant a_0 increases linearly with increasing Cr concentration from starting value of 8.45 ± 0.004 Å for $Co_{0.5}Zn_{0.5}Fe_2O_4$ to 8.60 ± 0.004 Å for $Cr_{0.5}Zn_{0.5}Fe_2O_4$ (Fig. 2). The trend of change in a_0 in ferrites with substitution of one cation with another is mainly due to cationic size effect.[16,17] Since Cr^{2+} has a larger ionic radius than Co^{2+}, substitution of Co with Cr would lead to an increase in a_0. The enhancement in the lattice constant in nanomaterials may also be attributed to the interface structure, which has a large volume fraction[18] in these materials. The decrease of grain size with addition of Cr therefore enhances surface effects in this series.

B. Mössbauer studies

Mössbauer spectra of $Cr_xCo_{0.5-x}Zn_{0.5}Fe_2O_4$ at 20 K are seen to be well resolved magnetic sextets (Fig. 3). The fitted parameters are given in Table I. The isomer shifts (IS) at 20 K at both A and B sites are seen to be almost a constant, which indicates that the s-electron distribution of the Fe^{+3} ions is insensitive to the Cr content. This is contrary to the trend of IS with Cr concentration observed at room temperature, where the IS at B site increases with increase in Cr

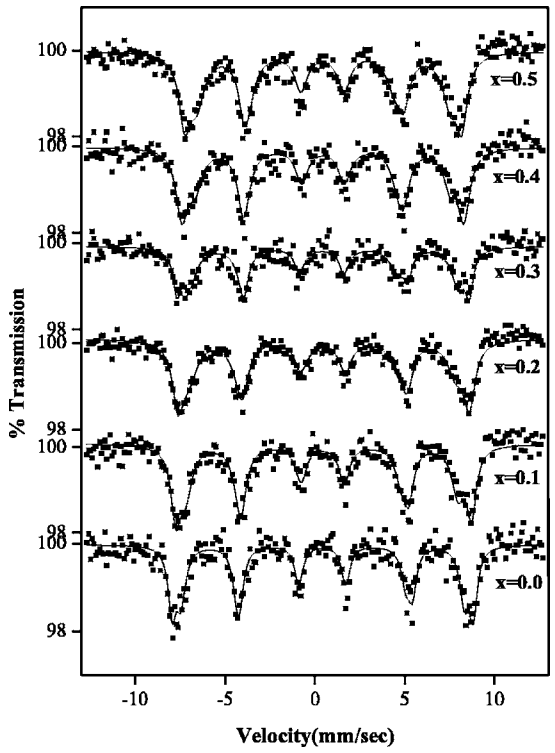

FIG. 3. Low-temperature Mössbauer spectra of the series $Cr_xCo_{05-x}Zn_{0.5}Fe_2O_4$ taken at 20 K.

concentration.[8] The IS value at 20 K is higher than that at 300 K by about 0.15 mm/s.

The isomer shift depends on temperature due to three different effects: the second-order Doppler shift (SOD), the change in the volume per atom resulting from thermal expansion, and the partial population of excited electronic states by thermal excitations. The second-order Doppler shift (SOD) is given by

$$\mathrm{SOD}(T) \approx \frac{-3kT}{2Mc}\left[1+\frac{1}{20}\left(\frac{\theta}{T}\right)^2\right]. \quad (3)$$

For ^{57}Fe, the change in IS due to SOD is about −0.0007 mm/s K.[19] The effect of change in the volume per atom due to thermal expansion is generally quite small and

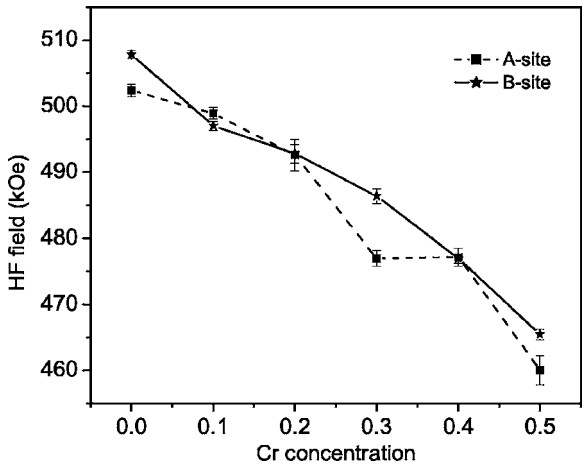

FIG. 4. Magnitude of hyperfine fields at ^{57}Fe nuclei at *A* and *B* sites.

can be of either sign. The third reason for the change in the isomer shift is the change in the electronic structure by thermal excitations.[20] This may cause a change in the isomer shift values of the order of ~0.0004 mm/s K in some cases. The value obtained in an experiment is the cumulative effect of all the three possible reasons. Since the difference between 20 K and RT is 280 K, the expected difference in IS values (assuming the change in isomer shift due to SOD as −0.0007 mm/s) is approximately 0.19 mm/s, which agrees fairly well with the observed difference in IS values of about 0.15 mm/s. The difference between the two may be due to the remaining terms.

The increase in IS values on replacement of all the Co with Cr is about 0.05 mm/s at the *B* site at room temperature. As pointed out earlier, at low temperatures, the IS seems to be insensitive to Cr content. The reason for this difference at RT and 20 K can be explained in terms of the decreased overlap between the ^{57}Fe nucleus and the *s*-electron wave function and hence an increase in IS due to some charge transfer from 4*s* to 3*d* orbital. At low temperatures, the available thermal energy is not enough to facilitate such a charge transfer.

Figure 4 shows the variation of hyperfine fields at *A* and *B* sites (H_A and H_B) in the nanosized samples with increasing Cr concentration at 20 K. The hyperfine fields at both crys-

TABLE I. Hyperfine field (HF), area under curve, isomer shift (IS), and FWHM of sextets (Γ) obtained by fitting the Mössbauer spectra at 20 K of $Cr_xCo_{0.5-x}Zn_{0.5}Fe_2O_4$.

Cr concentration (x)	HF field (kOe)		Area (%)		IS[a] (mm/s)		Γ (mm/s)	
	A	*B*	*A*	*B*	*A*	*B*	*A*	*B*
0.1	498.8±1.0	497±0.7	23.9±3.5	76±4.4	0.32±0.01	0.48±0.01	0.39±0.03	1.06±0.02
0.2	492.6±2.4	492.8±1.4	23.8±4.2	76.2±5.3	0.33±0.04	0.48±0.02	0.57±0.04	1.1±0.02
0.3	476.9±1.2	486.3±1.1	22.5±5.2	77.5±2.8	0.32±0.02	0.48±0.02	0.43±0.01	1.13±0.007
0.4	477.1±1.4	476.9±0.8	23.4±5.3	76.6±2.1	0.32±0.02	0.47±0.01	0.45±0.02	1.02±0.01
0.5	460±2.2	465.4±0.8	26.5±5.5	73.4±2.4	0.32±0.03	0.46±0.01	0.54±0.01	1.16±0.02

[a]IS values are with respect to metal iron.

TABLE II. Cation distributions in spinel structure of $Cr_xCo_{0.5-x}Zn_{0.5}Fe_2O_4$.

x	A site	B site
0.0	$Cr_{0.0}Co_{0.04}Zn_{0.5}Fe_{0.46}$	$Cr_{0.0}Co_{0.46}Zn_{0.0}Fe_{1.54}$
0.1	$Cr_{0.0}Co_{0.02}Zn_{0.5}Fe_{0.48}$	$Cr_{0.1}Co_{0.38}Zn_{0.0}Fe_{1.52}$
0.2	$Cr_{0.0}Co_{0.02}Zn_{0.5}Fe_{0.48}$	$Cr_{0.2}Co_{0.28}Zn_{0.0}Fe_{1.52}$
0.3	$Cr_{0.0}Co_{0.05}Zn_{0.5}Fe_{0.45}$	$Cr_{0.3}Co_{0.15}Zn_{0.0}Fe_{1.55}$
0.4	$Cr_{0.0}Co_{0.03}Zn_{0.5}Fe_{0.47}$	$Cr_{0.4}Co_{0.07}Zn_{0.0}Fe_{1.53}$
0.5	$Cr_{0.0}Co_{0.0}Zn_{0.47}Fe_{0.53}$	$Cr_{0.5}Co_{0.0}Zn_{0.03}Fe_{1.47}$

tallographic sites for sample with $x=0.0$ are almost equal and are consistent with reported values.[21] On increasing x, i.e., Cr concentration, the hyperfine fields at both sites are seen to decrease. Cr ions are known to have a strong preference for the octahedral B site in ferrites. RT Mössbauer studies on the same samples[8] have also clearly shown that in the present series on substitution of Co with Cr, Cr goes into the octahedral B sites. Estimate of the cation distribution in the present series (Table II) has been made on the basis of area occupied by Fe ions at A and B sites obtained from Mössbauer data. Since there are four cations involved, the relative strength of preference of occupation of sites has been taken into consideration while making this distribution. Accordingly, Zn has been assigned to the tetrahedral A sites first and Co is assigned to the tetrahedral site rather than Cr when necessary, since Cr is known to have a stronger octahedral site preference.

The crystal structure of ferrites plays a key role in determining their properties. Hence, the lattice constant a_0, oxygen parameter u, tetrahedral and octahedral bond lengths, tetrahedral edge, and shared and unshared octahedral edges for the series calculated theoretically from the cation distribution would provide a better insight into the observed hyperfine parameters.

The mean ionic radius of tetrahedral A sites (r_A) and of the octahedral B sites (r_B) can be calculated using the expressions[22,23]

$$r_A = \{[1-(x+y)]r_{tetra\ Fe^{+3}} + xr_{tetra\ Co^{+2}} + yr_{tetra\ Zn^{+2}}\}, \quad (4)$$

$$\{[1+(x+y)]r_{oct\ Fe^{+3}} + (0.5-x-z)r_{tetra\ Co^{+2}} + (0.5-y)r_{tetra\ Zn^{+2}} + zr_{oct\ Cr^{+2}}\}, \quad (5)$$

where x and y are the concentrations of Co^{+2} and Zn^{+2} ions at tetrahedral A sites, respectively, and z is the concentration of Cr^{+2} ions at octahedral B sites. The theoretical lattice parameter a_{th}, given in Table III, calculated from the relation[24]

$$a_{th} = (8/3\sqrt{3})[r_A + R_O] + \sqrt{3}[r_B + R_O], \quad (6)$$

where R_O is the radius of oxygen ion, follows the same trend as that obtained experimentally, supporting the estimated cation distribution.

Using the values of a_{th}, R_O, and r_A in the following expression, the value of the oxygen parameter u is calculated (Table III) from the equation

TABLE III. Calculated parameters: mean ionic radius of tetrahedral A sites (r_A) and octahedral B sites (r_B), theoretical lattice constant a_{th}, and oxygen parameter u.

Cr concentration (x)	r_A (Å)	r_B (Å)	a_{th} (Å)	Oxygen parameter u (Å)
0.0	0.707	1.363	8.548	0.3965
0.1	0.706	1.376	8.569	0.3961
0.2	0.706	1.388	8.590	0.3957
0.3	0.7075	1.3985	8.611	0.3955
0.4	0.7065	1.4115	8.632	0.3951
0.5	0.7029	1.4271	8.652	0.3945

$$r_A = (u-1/4)a_{th}\sqrt{3} - R_O. \quad (7)$$

The tetrahedral and octahedral bond lengths (d_{AX} and d_{BX}), tetrahedral edge (d_{AXE}), and shared and unshared octahedral edges (d_{BXE} and d_{BXEU}) have also been calculated as follows:[25,26]

$$d_{AX} = a_{th}\sqrt{3}(u-1/4), \quad (8)$$

$$d_{BX} = a_{th}[3u^2 - (11/4)u + 43/64]^{1/2}, \quad (9)$$

$$d_{AXE} = a_{th}\sqrt{2}(2u-1/2), \quad (10)$$

$$d_{BXE} = a_{th}\sqrt{2}(1-2u), \quad (11)$$

$$d_{BXEU} = a_{th}[4u^2 - 3u + (11/16)]^{1/2}. \quad (12)$$

The calculated values, plotted in Fig. 5, show that with an increase in Cr concentration, the tetrahedral bond length and tetrahedral edge remain nearly a constant, the octahedral bond length and shared octahedral edge increase, and the unshared octahedral edge shows a very small increase. These results point to the fact that the larger Cr ions replace Co ions at the octahedral B site. The oxygen parameter u is a quantitative measure of the displacement of an oxygen ion due to substitution of a metal cation into the tetrahedral (A) site. In an ideal fcc structure, $u=3/8=0.375$. Although most ferrites generally have u greater than this ideal value,[1] it is much larger in the present series (Table III), implying that the oxygen ions are displaced in such a way that in the A-B interaction, the distance between A and O ions is increased while that between B and O is decreased. This leads to a decrease in the A-A interaction and an increase in the B-B interaction.

In ferrites, if the metal ions occupying the tetrahedral (A) and octahedral (B) sites possess a magnetic moment, cooperative (ferrimagnetic) behavior is observed due to the antiferromagnetic A-B superexchange interaction mediated by oxygen ions. In general, since these interactions are indirect and the nearest neighbors of cations at A sites are the cations at B site and vice versa, the A-B superexchange is the strongest one. The hyperfine magnetic field at the A/B sites is a function of the cation distribution at the nearest neighbor

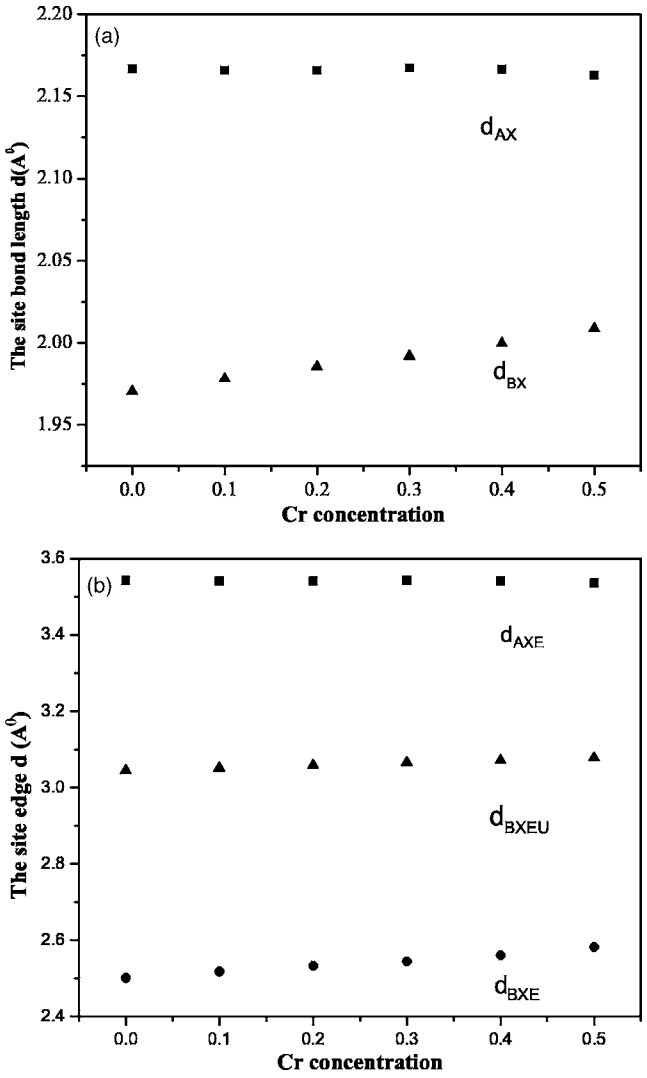

FIG. 5. (a) Effect of Cr substitution on tetrahedral (d_{AX}) and octahedral (d_{BX}) bond lengths. (b) Effect of Cr substitution on tetrahedral edge d_{AXE}, shared d_{BXE}, and unshared d_{BXEU} octahedral edge.

B/A sites. In nanosized $Cr_xCo_{0.5-x}Zn_{0.5}Fe_2O_4$, the magnetic hyperfine fields at low temperatures at the A and B sites have nearly the same values for all concentrations of Cr with a consistent decrease in the value of hyperfine fields at both sites with increasing Cr concentration. The hyperfine field at the A site is due to the net magnetization of the nearest neighbor B site through A-B superexchange and the very weak A-A interaction. Since Cr moments order antiferromagnetically with the magnetic moments of Fe ions, substitution of Cr into the B site reduces the magnetization at the B site. Consequently, the hyperfine field at the A site decreases. The two types of interactions responsible for the hyperfine fields at the B sites are the A-B and B-B types. Table II shows that the configuration of A sites does not change very much across the series, and therefore, any change in the hyperfine field at the B site cannot be explained in terms of a change in configuration of the nearest neighbor. The next-nearest neighbor to a B site cation is another B site cation, and so the observed systematic decrease in the hyperfine field at the B site with increase in Cr concentration is due to the B-B exchange interaction. Moreover, as observed, not only is the trend of change in hyperfine field at B site the same as that at A site, the change in actual intensities are also nearly the same. This points to a stronger B-B interaction in this series than is usual in most ferrites. The calculated value of the oxygen parameter u, which is larger than its ideal value, also supports this conclusion.

The trend of hyperfine fields at the A and B sites in the bulk series of the same composition is very different from that in the corresponding nanosamples. In the bulk samples, H_B is smaller than H_A and reduces drastically with increase in Cr concentration. The value of H_A remains nearly constant with Cr content, contrary to the trend observed in nanosamples where both H_A and H_B are nearly equal and both reduce at an almost equal rate on addition of Cr. The trend of hyperfine fields at the A and B sites in bulk samples has been explained in terms of quenching of the A-B interaction,[7] whereas the A-B and B-B interaction together contribute to the hyperfine fields in nanosamples.

In conclusion, low-temperature Mössbauer studies on nanosamples of $Cr_xCo_{0.5-x}Zn_{0.5}Fe_2O_4$ corroborate the results of RT Mössbauer measurements done on these samples and show that Cr enters preferentially into the B site on substitution with Co. Theoretically calculated values of the lattice parameter support the cation distribution estimated from fitted Mössbauer parameters. The high value of the calculated oxygen parameter u satisfactorily explains the observed trends of magnetic hyperfine fields at the B site on Cr substitution.

ACKNOWLEDGMENTS

This work has been supported by the UGC-DRS and DST-FIST schemes of the Department of Physics, Mohanlal Sukhadia University, Udaipur. We thank D. M. Phase, UGC-DAE CSR, Indore, for the EDX measurements. One of us (R.K.S.) acknowledges financial support by CSIR.

[1] J. Smit and H. P. J. Wijn, *Ferrites* (Philips Technical Library, Eindhoven, 1959).
[2] C. N. Chinnasamy, A. Narayanasamy, N. Ponpandian, and K. Chattopadhyay, Mater. Sci. Eng., A **304–306**, 983 (2001).
[3] C. Rath, S. Anand, R. P. Das, K. K. Sahu, S. D. Kulkarni, S. K. Date, and N. C. Mishra, J. Appl. Phys. **91**, 2211 (2002).
[4] K. Mandal, S. Chakraverty, S. P. Mandal, P. Agudo, M. Pal, and D. Chakravorty, J. Appl. Phys. **92**, 501 (2002).
[5] T. T. Ahmed, I. Z. Rahman, and M. A. Rahman, J. Mater. Process. Technol. **153–154**, 797 (2004).
[6] M. V. Kuznetsov, L. F. Barquin, A. Pankhurst, and I. P. Parkin, J. Phys. D **32**, 2590 (1999).

[7] R. K. Sharma, O. P. Suwalka, N. Lakshmi, and K. Venugopalan, Hyperfine Interact. **165**, 261 (2005).
[8] R. K. Sharma, O. P. Suwalka, N. Lakshmi, K. Venugopalan, A. Banerjee, and P. A. Joy, Mater. Lett. **59**, 3402 (2005).
[9] M. Calligaris and S. Geremia, PDP, powder diffraction package, Version 1.1, ICTP, SMR/455-1, 1990.
[10] E. von Meerwal, Comput. Phys. Commun. **9**, 117 (1975).
[11] R. F. Strickland-Constable, *Kinetics and Mechanism of Crystallization* (Academic, New York, 1968).
[12] A. Navrotsky and O. J. Kleppa, J. Inorg. Nucl. Chem. **30**, 479 (1968).
[13] J. Wang, C. Zeng, Z. Peng, and Q. Chen, Physica B **124–128**, 349 (2004).
[14] R. Velenzuela, *Magnetic Ceramics: Chemistry of Solid State Materials* (Cambridge University, New York, 1994).
[15] C. Upadhyay, H. C. Verma, C. Rath, K. K. Sahu, S. Anand, R. P. Das, and N. C. Mishra, J. Alloys Compd. **326**, 94 (2001).
[16] B. P. Ladgaonkar, P. N. Vasambekar, and A. S. Vaingakar, J. Magn. Magn. Mater. **210**, 289 (2000).
[17] G. Chandrasekaran and P. Nimy Sebastian, Mater. Lett. **37**, 17 (1998).
[18] D. Anderson, L. M. Roberto, N. D. S. Mohallem, and A. S. Persiano, J. Magn. Magn. Mater. **172**, L9 (1997).
[19] G. K. Shenoy and F. E. Wagner, *Mössbauer Isomer Shift* (North-Holland, Amsterdam, 1978).
[20] T. Komatsu and N. Soga, J. Appl. Phys. **51**, 5926 (1980).
[21] B. K. Nath, P. K. Chakrabarti, T. Roy, S. K. Brahama, S. Das, U. Kumar, P. K. Mukhopadhyay, and D. Das, Proceedings of DAE Solid State Physics Symposium, Gwalior, India, 26–30 December 2003 (unpublished), Vol. 46, p. 231.
[22] M. A. Amer and M. E. Hiti, J. Magn. Magn. Mater. **234**, 118 (2001).
[23] O. Ravinder, J. Appl. Phys. **75**, 6121 (1994).
[24] A. A. Yousef, M. E. Elzain, S. A. Mazen, H. H. Sutherland, M. A. Abdallah, and S. F. Mansour, J. Phys.: Condens. Matter **6**, 5717 (1994).
[25] C. Arean, J. Blanco, J. Gonzles, and M. Fernandez, J. Math. Psychol. **9**, 229 (1990).
[26] T. Abbas, Y. Khan, M. Ahmad, and S. Anwar, Solid State Commun. **82**, 710 (1992).